Hybrid FuzzyPCA-VGG16 Framework for Classifying Pox Virus Images

K.P. Haripriya
Department of Computer Science, Periyar University
India
priya22prakasam@gmail.com

H. Hannah Inbarani
Department of Computer Science, Periyar University
India
hhinba@periyaruniversity.ac.in

Abstract: *Classifying similar disease characteristics can be challenging, especially when multiple classes are involved. Classifying conditions with multiple classes is riskier. Early and accurate disease detection enables the physician to treat the case appropriately. In a real-world scenario, classifying a similar type of disease is essential. Recently, researchers implemented deep learning approaches to classify images of the pox virus. Pre-trained models are commonly used to classify the disease. However, medical images contain significant noise and uncertain information, complicating the classification process. Different deep learning approaches such as Convolution Neural Network (CNN), Visual Geometry Group (VGG16), and Resnet50 were applied for the classification of pox virus images. In this research work, VGG16 produces better results in generalization. So, the VGG16 method is taken for improvement. The VGG-16 approach often leads to overfitting and incorrect data classification. To solve this problem, we incorporated two primary functions into the VGG16 models, which are as follows: Initially, we employed fuzzy functions to manage uncertainty and Principal Component Analysis (PCA) to reduce dimensionality. We compare the hybrid FuzzyPCA-VGG16 model with other benchmark methods for classification, this method minimizes the overfitting. The experimental results show a significant improvement over other model. The hybrid FuzzyPCA-VGG16 method attains 97.14% accuracy in binary classification and 91.42% in multi-class classification. The proposed work significantly improves the classification report for both binary and multi-class classification. This approach supports early and accurate disease classification.*

Keywords: *Classification, VGG-16, PCA, fuzzy membership function, CNN, resnet50, data augmentation.*

Received August 14, 2024; accepted April 8, 2025
https://doi.org/10.34028/iajit/22/3/14

1. Introduction

Classification is critical in the identification of diseases caused by pox viruses. Although binary classification is straightforward, multi-class classification of diseases with similar symptoms is an exciting challenge. In 2021, the world responded to the COVID-19 pandemic, demonstrating its resilience and adaptability. Likewise, pre-emptive measures to tackle the increasing threat of monkeypox, which originated in the Congo region, have demonstrated the significance of sophisticated diagnostic instruments. Accurate differentiation of identical kinds of skin lesions leads to opportunities for new answers in health care. Since the monkeypox virus originated in Africa, it is the cause of the monkeypox disease [11]. The virus first began to spread over the central and west of the nation. According to the author [34], monkeypox is the cause of the world's problems and is easily spread between humans and animals. Currently, there is a monkeypox outbreak in the Congo in 2024. From January to April of 2024, the Conga reported 4500 suspected cases; of those, roughly 300 instances resulted in death [43]. The absence of distinct symptoms, such as headaches, myodynia, shivering, fever, fainting, and backaches, complicates accurate diagnosis. However, one of the most prevalent signs of monkeypox, lymphatic hyperplasia, may help identify the illness [23]. The normal incubation period of monkeypox disease is 21 days. The varicella-zoster virus, which causes chickenpox, is the next family of diseases [7]. It primarily affects children; however, it can also strike adults. The virus first appears as a tiny rash, but after a while, it develops into rashes that are fluid-filled. Once the virus gets affected in the human body, it causes severe irritation, which has caused it to spread across every area of the body. For this condition, the typical incubation period is between 10 to 21 days. Early on, individuals may have a high temperature, tiredness, discomfort in the joints, headaches, and, in rare cases, respiratory system complications.

The next class is the measles virus [29], a member of the morbillivirus family, which primarily affects children. A person with a weakened immune system immediately impacts our neurological system. After the virus enters our bodies, the illness typically takes 10 to 14 days for incubation [19]. If the virus is not eliminated from our bodies, the virus will start to manifest its effects after two or three years. It continuously spreads through intercourse, close contact with infected individuals, or through the air, and it begins to spread in densely populated areas.

These three kinds of viruses look similar in the early

stages, so it is quite difficult to distinguish between them when the red bumps overlap in a picture. To classify these images, deep learning techniques, notably Convolutional Neural Networks (CNNs), work well for binary classification but are ineffective for multiclass classification. This is why pre-trained models in medical image processing have started to appear. In the pre-trained models, generalization of similar skin lesions is quite difficult even though it was extracting the global features. To address this issue, fuzzy and PCA techniques were used to enhance the classification accuracy and robustness. This study proposes a novel hybrid method of Fuzzy Principal Component Analysis (FuzzyPCA) VGG16 which integrates fuzzy triangular membership and PCA with Visual Geometry Group (VGG16) architecture are applied to classify the images based on the above challenges. To address the overfitting issues, batch normalization, dropout, and data augmentation techniques are used.

This research endeavours to develop a precise and efficient classification model for pox virus diseases, thereby addressing the overlapped features in multi-class classification and overfitting in deep learning models. The introduction of the fuzzy Membership Function (MF) and PCA integrated hybrid model, FuzzyPCA-VGG16, aims to enhance classification accuracy while maintaining robustness. The ultimate end is the improvement of disease detection at an early stage, thereby mitigating the mortality and morbidity factors, particularly in children. The suggested methodology includes preprocessing of medical images, employing PCA for dimensionality reduction, and utilising the fuzzy triangular MF for class classification.

This paper presents the following key contributions: The classification of the pox virus is crucial in the initial stage. The automated classification is done based on deep learning techniques by using VGG16, CNN, Resnet50, and the proposed work of HybirdNet FuzzyPCAVGG16. Implementation of dropout, batch normalization, and data augmentation to mitigate overfitting. Achievement of high accuracy in multi-class (91.42% testing) and binary classification, outperforming existing methods.

The following is the paper's structure: Section 2 provides varying perspectives from authors regarding the pox virus identification and the deep learning technique currently in use. Section 3 provides a full discussion of the proposed novel work and the suggested techniques. Section 4, discusses the evaluation metrics and their findings. The work's conclusion and future projects about this topic are covered in section 5.

2. Relevant Works

To identify diseases as quickly as possible, automated method-based classification of medical images has recently begun to flourish. Deep learning-based classification methods are now very useful in illness prediction. This section will cover many deep-learning approaches used to predict the pox virus and other datasets.

Sahin *et al*. [39] propose a pre-trained deep-learning approach for the detection of the human monkeypox virus. The author obtained the dataset from the Kaggle website, utilizing publicly accessible data to enhance the images. Every image is then subjected to a deep learning algorithm, such as ResNet 18, GoogleNet, EfficientNetb0, ShuffleNet, MobileNetv2, and Nasnet Mobile, after augmentation. Of these, MobileNetv2 and EfficientNetb0 attained an accuracy of 91.11%. Eventually, a smartphone app for locating skin lesions caused by human monkeypox has been created. To classify the human monkeypox virus and other viruses, the author first proposed the feature selection approach [1] and subsequently used the Neural Network (NN) method. They performed classification both with and without the feature selection method, which yielded satisfactory results. The recommended feature selection techniques were the hybrid Particle Swarm Optimization (PSO) and Al-Biruni Earth Radius (BER) as an optimization algorithm; 93.11% had the highest scores. The author employed ensemble approaches, ResNet50, VGG-16, InceptionV3, and other deep learning pre-trained models to identify skin image problems and the monkeypox virus to recognize photos of skin lesions. The author used three-fold cross-validation to partition the dataset into 70% for training, 10% for validation, and 20% for segment testing. ResNet50 produced good findings, with 82.96% [5]. According to Ahsan *et al*. [3], the modified VGG-16 yields good results for binary prediction of images of the pox virus, including monkeypox. They introduce the Local Interpretable Model-agonistic Explanations (LIME) approach for classification in the upgraded VGG-16. For primary predictions, this method is particularly helpful as it typically isolates the main features from the images, acting as a super-pixel. One of these two studies discusses the original image, while the other discusses the augmented imagery. Study 1 yields an accuracy rate of 97% in general.

The skin lesion dataset from Kaggle that was used by Sitaula and Shahi [42] was monkeypox-related. Ensemble methods, VGG16, VGG19, Resnet-50, ResNet-101, IncepResNetv2, MobileNetV2, InceptionV3, Xception, EfcientNet-B0, EfcientNet-B1, EfcientNet-B2, DenseNet-121, and DenseNet-169 are among the previously taught deep learning techniques that are employed in this. It performs well when Xception and DenseNet-169 are combined for multi-class classification. Before using the deep learning techniques, the data augmentation and the k-fold cross-validation (5-fold) are applied. The ensemble method produces 87.13%. Under the tag of poxNet22, Yasmin *et al*. [47] provide the enhanced Inception V3 technique. This methodology employs multiple layers, such as

global average pooling, batch normalization, and data augmentation, to mitigate overfitting issues. They experimented with many deep learning techniques to find the optimal strategy before deciding on the Inception V3 method. They both performed with and without augmentation, producing 100% and 97% of the results, respectively, with augmentation.

Albashish *et al*. [4] investigate the classification of breast cancer using a VGG16-based deep CNN. The dataset comes from the eight main classes of histopathological pictures seen in the BreaKHis breast cancer dataset. From VGG-16, the author retrieved the features. Following feature extraction, machine learning-based classification algorithms including Support Vector Machine (SVM), NN, Logistic Regression (LR), and K-Nearest Neighbour (KNN) are applied. Radial Basis Function (RBF) and Poly are the kernels that are utilized in kernel-based categorization in SVM. The classification techniques are used for both multi-class and binary classification. Radial Basis Function-Support Vector Machine (RBF-SVM) received an equivalent of 89.33% for multi-class classification. Barhoom *et al*. [9] investigate the deep learning pre-trained models to predict and classify bone abnormalities. The author of this paper employed XR images of fourteen different classes of bones, including the humerus, wrist, forearm, elbow, finger, and hand. To identify and categorize bone anomalies, they created a modified version of the VGG-16 approach and compared it to the original. In terms of multi-class categorization, they scored 85.77%. To classify images of diabetic retinopathy, Da Rocha *et al*. [14] employed three distinct kinds of datasets. Three distinct dataset types are used to apply the VGG-16 classification algorithm: DDR, EyePACS from Kaggle, and IDRID (Indian Diabetic Retinopathy Image Dataset). The suggested method yields good accuracy for DDR picture datasets, with an accuracy rate of 85.94%. Krishnaswamy Rangarajan and Purushothaman [27] figured out how to identify illness in eggplants. There are five distinct classifications in which eggplant illness can manifest itself. It can be caused by fungi, viruses, or natural causes. For color, grayscale, Hue Saturation Value (HSV), and YCbCr images, the pre-trained VGG16 classification techniques are used. Several classification algorithms, including AlexNet, GoogleNet, VGG-16, ResNet101, and DenseNet 201, are used. Both laboratory and field conditions are used to screen for eggplant disease. For the VGG16 method, both approaches yield good results, with respective percentages of 99.4%.

According to Kavitha and Inbarani [26], the hybrid approach combining CNN with the Bayes wavelet transform yields good results, with 97.7% in the 20th epoch, respectively. They used the COVID and chest X-ray pictures as their datasets. The imagery is first denoised using the Bayes wavelet transform method, and subsequently, they are used to implement the 8-layer CNN algorithm for classification. A good result of 95% will be obtained, according to Nivetha and Hannah Inbarani [33] examination of the rough set-based classification algorithm. To distinguish between normal and abnormal states, the deep approach was used as Deep Tolerance Rough Set (DTRS) and Novel Tolerance Rough Set (NTRS) after the author retrieved the Gray Level Co-occurrence Matrix (GLCM) features from a Computed Tomography (CT) scan of lung images. The disease known as monkeypox is predicted using a variety of machine-learning algorithms, as reported by Haripriya and Hannah Inbarani [21]. The author computed binary predictions using a Kaggle Comma-Separated Values (CSV) dataset. To achieve good results, the author performed ranker-based feature selection before applying machine learning techniques. Gradient Boosting (GB) produces better results than other machine learning approaches, such as KNN, Naive Bayes (NB), Random Forest (RF), SVM, LR, Ada Boosting (AB), GB, and Decision Tree (DT) methodologies; their respective accuracy was 71%. An image of the pox virus was taken from the Kaggle website by Haripriya and Hannah Inbarani [22]. The author used wavelets with GLCM, Local Binary Pattern (LBP), and Haralick features as a technique to extract texture and shape-based characteristics from images. After the features have been retrieved, machine learning-based classification models are used to identify which feature extraction methods are most effective in categorizing pox virus infections. A variety of machine learning algorithms are used, including AB, GB, KNN, SVM, RF, and NB. When compared to other methods, wavelets merged with GLCM yield superior results when applied to gradient-boosting machine learning-based algorithms. 84.41% is the outcome that is produced, correspondingly. Gunasekaran and Vivekasaran [20] execute the multi-class categorization approach. The author investigates the fetal heart blood vessels in the chest x-ray scan images. For these, CNN CNN-based model was used for classification to diagnose the disease.

This section highlights the extensive use of binary classification approaches for pox virus detection in deep learning, showing their effectiveness in achieving high accuracy. In addition, a growing number of studies are exploring multi-class predictions, demonstrating the potential for deep learning to handle more complex classification tasks.

Deep learning algorithms have been applied to eggplant, iris illness, bone disease, and brain pictures, proving their versatility and adaptability in medical and agricultural fields.

3. Materials and Methods

As depicted in Figure 1, the architecture elucidates the entire scope of this article. Images of the pox virus with four distinct class labels are used as input; the color

image is taken for preprocessing. To address the overfitting and underfitting issues, data augmentation and image normalization are done. Image normalization modifies the range of intensity values, and it is a challenging step in medical image processing. The training, validation, and testing data are divided into 70-10-20 ratios. Deep learning methods such as VGG16, CNN, and Resnet methods are applied. Based on the values of evaluation measures, the suitable model to classify the pox virus images can be found. From this, the improved model can be developed.

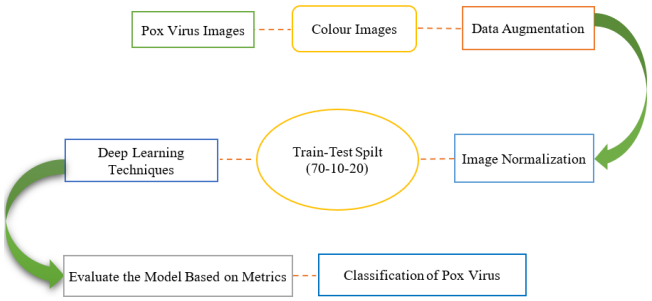

Figure 1. The work's general architecture data augmentation.

3.1. Preprocessing

3.1.1. Augmentation of Image

Augmentation of images is a technique that uses data augmentation parameters to artificially enhance the amount of data. To prevent overfitting data augmentation is one of the methods. So, overfitting [6] relates to excellent results on training data but weak results on test or validation data for generalization, and in the same way under-fitting relates to weak performance in training but provides excellent results on test or validation data for generalization. Different types of augmentation techniques are available such as Traditional-based augmentation, and deep learning-based augmentation [30].

Again, traditional-based augmentation is subdivided into different types, such as geometric transformation, random erasing, kernel filters, and color space transformation. By moving individual picture pixels from their original locations to new locations while maintaining the pixel values, geometric transformation modifies the geometrical structure of images.

It will also discuss the various geometrical augmentations and the "safety" of utilizing them. Safety is the likelihood that a data augmentation technique would preserve the label following transformation [41]. Geometric augmentation has two types: Affine image transformation and non-affine transformation.

In affine image transformation [31] performs different operations such as rotation, flip, translation, scaling, cropping, and shearing.

Rotating an image concerning its initial position yields rotation-based image augmentations. While employing a new coordinate system, the rotation maintains the relative positions of the image's pixels. It may move across an axis in either a right or left direction between [1° and 359°]. Rotation transformation is generally safe for medical images [18]. The image is typically flipped in one of three directions: horizontally, vertically, or both. Scaling involves frequently performing zoom-in or zoom-out operations, which increase or reduce the size of the image [46]. The parameters utilised for picture augmentation are covered in Table 1.

Table 1. Parameter used in the augmentation of image.

Parameter name	Parameter size
Range of rotation	40
Range for width_shift	0.3
Range for height_shift_	0.3
Range of shear	0.3
Range of zoom	0.3
horizontal_flip	True
vertical_flip	True
fill_mode	Nearest
featurewise_center	false
samplewise_center	false
Normalization of featurewise_std	false
Normalization of samplewise_std	false
preprocessing_function	None
rescale	None
zca_whitening	false
zca_epsilon	0

3.1.2. Image Normalization

In deep learning, image normalisation is crucial as it rescales pixel values to a standard range, often between 0 and 1 or -1 and 1 [12, 28]. By default, we have min-max normalization to implement this rescaling. Constraints of input values within the appropriate range make the model train better with fewer complications such as exploding and vanishing gradients at the backpropagation process. The min-max normalization equation is given in Equation (1).

$$X' = \frac{(X - X_{\min})}{(X_{max} - X_{min})} \tag{1}$$

X' denotes the normalized value of the image, X denotes the original pixel value, X_{min} signifies the least pixel value in the image, and X_{max} indicates the maximum pixel value in the image.

3.2. VGG16

A kind of pre-trained CNN is the VGG-16. It is a well-liked technique in computer vision, and ImageNet took up the top honour in 2014 [16]. It provides good accuracy results for tiny datasets. VGG-16 consists of 13 layers of convolution with 3*3 filters, immediately following 5 pooling layers. The prediction of the pox virus is derived from two fully connected layers utilising relu as the activation function, succeeded by a dense layer employing soft-max as the activation function [44]. Figure 2 explains the architecture of VGG16.

The problem with VGG16 [25] is related to feature extraction from medical images. In the beginning, the ImageNet Large-Scale Visual Recognition Challenge (ILSVRC) employed VGG16 to recognize 1000

categories from a million images. Consequently, there was a noticeable overfitting issue when it was applied to tiny datasets with fewer training characteristics. The features of an image are uniform and ambiguous. Thus, extracting appropriate data from the dataset is challenging.

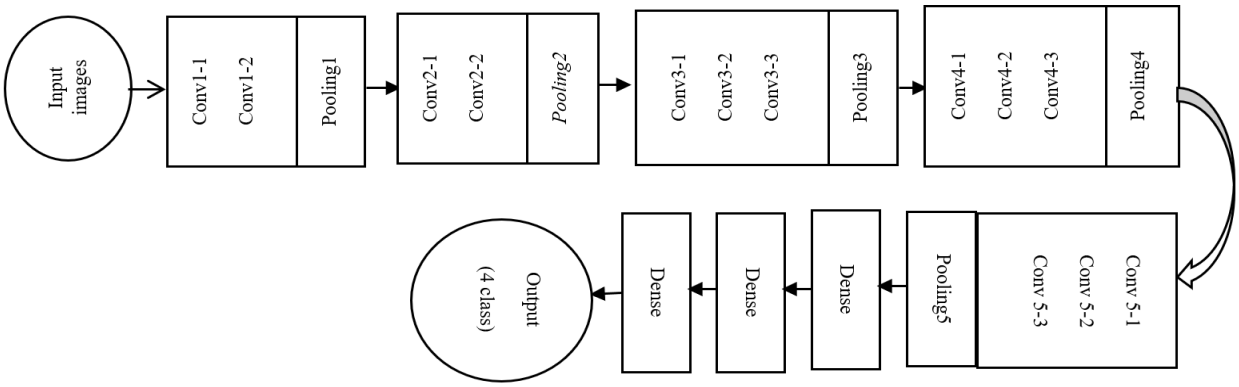

Figure 2. The architecture of the VGG16.

3.3. CNN

CNNs [2] process an input image; the convolutional layer utilises filters to extract spatial and temporal characteristics, succeeded by another convolutional layer and a max pooling layer. The maximum values are selected according on the kernel size. The objective is to extract the pertinent features. This study included five convolutional layers succeeded by max pooling layers. Subsequent to flattening the feature values, implement a dense layer. The final classification was executed in the dense layer utilising the SoftMax activation algorithm.

3.4. Resnet50

ResNet-50 [40] is a deep CNN architecture trained on extensive datasets of natural pictures. It has demonstrated efficacy in numerous computer vision applications, including picture classification, object detection, and semantic segmentation. ResNet-50, a variant of the ResNet architecture that triumphed in the ILSVRC in 2015, is highly effective for transfer learning in medical imaging applications, such as pox virus image categorisation. The ResNet-50 architecture uses residual connections, which solve the problem of vanishing gradients and are able to train deeper networks. It is composed of 50 layers of operations of convolution and pooling distinguished by its ability to make it possible for gradients to flow smoothly through the network, thus making it converge more rapidly and learn better [35].

3.5. Proposed Method

3.5.1. FuzzyPCA-VGG16 Hybrid Net

Figure 3 discusses the construction of the FuzzyPCA-VGG16 Hybrid Net. The VGG-16 model's convolution layer freezes in this workflow because it typically collects spatial characteristics from images, such as texture, edges, and shapes. To make the feature maps smaller, pooling layers and 3*3 filters are employed. The FuzzyPCA hybrid net that was produced after the frozen layers were computed is shown in Figure 5. The output of the hybrid net is retrieved and input into a fully integrated NN for the classification of pox virus infection. To stop the network from overfitting, batch normalization and the dropout layer are employed. The following describes other parameters.

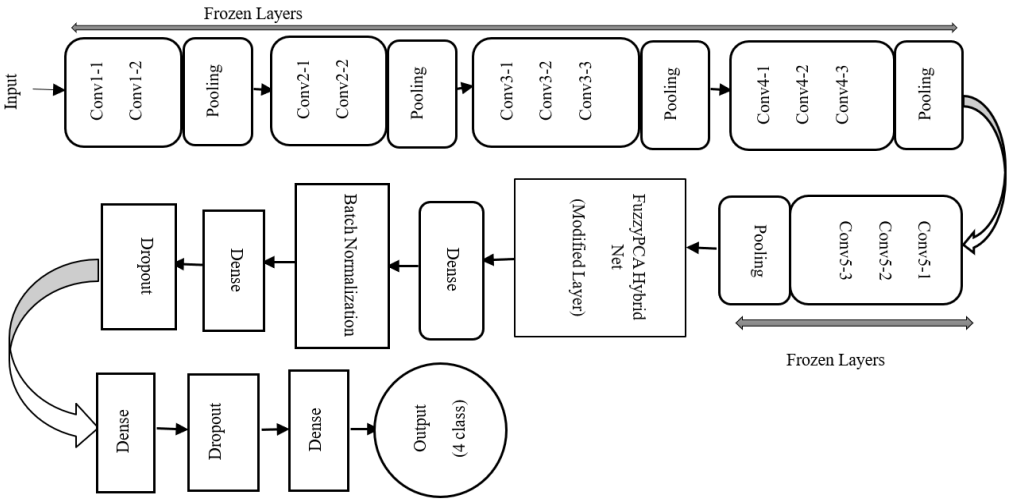

Figure 3. The workflow of proposed work.

- **Batch Size**: batch size of the layer as 32
- **Epoch**: the network was trained for different epochs as 30,50,100. In that 100 epoch, it produces a good result.
- **Optimizer**: Adam optimizer was used and it produced a good result.
- **Loss**: The loss function was calculated using the classification with binary values as binary_cross entropy approach, and the classification with multiple classes categorical_cross entropy loss function was used to forecast it.
- **Early Stopping**: it is critical to halt the network early to address the overfitting problems. Based on the "validation loss" the epoch will continue continuously if the loss is decreasing, and it will stop if the loss is increasing. The multi-class classification approach used a 100 epoch, while the binary classification method used a 74 epoch for stopping.
- **Batch Normalization**: Batch Normalisation (BN) converts the input distribution into a normal distribution with a zero mean and one variance. After this conversion, the distribution falls within the activation function's sensitive interval, meaning that even small input changes can drastically affect the loss function. Additionally, by increasing the gradient, the issue of gradient dispersion is avoided. Deep neural networks will converge more quickly due to the bigger gradient, which can significantly speed up the training process [24, 45].
- **Dropout**: Dropout [17] is a method for minimizing overfitting. Its main concept is to train sub-models resulting from an overfitting model by randomly dropping units for each training batch. The dropout's size is fixed at 0.1. Dropout enables the unit to become more resilient by continuously removing random units, allowing it to learn independently of other units.
- **Principal Component Analysis (PCA)**: PCA is the technique that is utilised for the decrease of dimensionality. The technique [8] of reducing the number of parameters taken into consideration is called dimensionality reduction. It can be applied to minimize the amount of data while preserving its structure or to extract latent properties from the unprocessed data. PCA [36] removes the vectors with the fewest variances in the dataset and arranges the resulting components so that the component with the greatest variance is at the top.

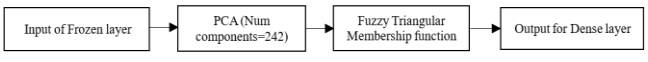

Figure 4. Number of components in PCA.

Figure 4 illustrates how to determine the appropriate number of components for an image threshold value, which is maintained at 96%. The predicted value is 24.

- **Triangular Membership Function**: a slope known as the MF [13] shows how each point on a scale of 0 to 1 corresponds to a membership degree. The scenario is graphically illustrated through the usage of MF. Systems using fuzzy logic handle both the degree of truth and the degree of membership. When handling the degree of uncertainty data in the pox virus images, the Triangular Membership Function (TMF) is employed. Typically, the TMF uses three parameters, such as p, q, and r, to assign values. A is worth zero, b is worth half, and c is worth one. Every class has a degree, and with the use of that degree, the class can be predicted. The TMF [37] can be computed using Equation (2), which is detailed below.

$$\mu(z) = \begin{cases} \dfrac{z-p}{q-p} & if\ p \le z < q \\ \dfrac{r-z}{r-q} & if\ q \le z \le r \\ 0 & if\ z > r \end{cases} \quad (2)$$

Algorithm 1: FuzzyPCA-VGG16 Hybrid Net.

Input: Images of the original Pox Virus
Output: Grouping of Pox Virus Images
Steps:

1. *Save a color image from the image file by opening it.*
2. *Include the VGG16 model, keeping the layers frozen. "ImageNet" makes up the VGG16 model's weights.*
3. *To transform VGG16's tensor output into a 1-dimensional image, add a flattened layer.*
4. *Perform PCA on the flattened result after adding PCA as a layer. Set the PCA's number of components counts to 242.*
5. *Include a layer for the fuzzy triangle membership function and initialize an instance with the given parameters (p=0, q=0.5, r=1).*
6. *To build a completely linked network on top of the feature extractor, add Dense Layers to the model.*
7. *Utilize the Relu activation function to account for non-linearity.*
8. *Add Batch Normalization layers to normalize the activation of the layer that came before it.*
9. *To prevent overfitting, incorporate dropout layers, which randomly eliminate some of the input units during training.*
10. *To generate class probabilities, use the SoftMax Activation Dense layer.*
11. *Finally classify the pox virus images.*

Figure 5 and Algorithm (1), discussed the FuzzyPCA Hybrid Net. The PCA component layer receives frozen layer input, reducing dimensionality and overfitting. Next, the extracted output is given as an input to the fuzzy TMF, which helps to handle the uncertainty. Now the fuzzy member function will generate a degree for each class. The dense layer is fed the extracted output as an input. Ultimately, the dense layer will classify the pox virus sickness using the SoftMax algorithm.

This section provides a comparative examination of various deep learning approaches with the suggested method, including a discussion of the learning parameter utilised for this approach. The subsequent part will detail the results and comparative analysis of the suggested work alongside the existing benchmark approach.

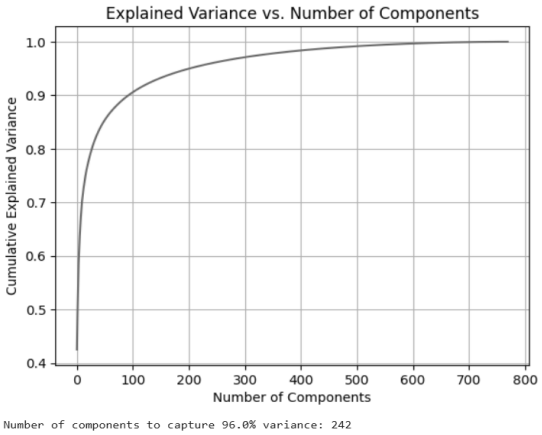

Figure 5. The FuzzyPCA hybrid net (modified layer).

4. Outcomes and Analysis

This section discusses the results for present methods such as VGG-16 and the suggested method, FuzzyPCA Hybrid Net.

4.1. Software and Hardware Specification

The experiment was conducted on a Windows platform utilising a robust 13th Gen Intel (R) Core (TM) i7-13620H processor at 2.40 GHz, complemented by 16 GB of RAM, which facilitated seamless performance for all computing workloads. The algorithms were developed using the versatile Anaconda platform along with the most robust packages like Scikit-Learn, Pandas, matplotlib, and Seaborn, TensorFlow, skfuzzy.

4.2. Dataset Description

Table 1 provides a summary of the dataset. The dataset, titled the Monkeypox Skin Image Dataset, is sourced from Kaggle [15]. The dataset comprises photos categorized into four class labels: chickenpox, measles, monkeypox, and normal. Each image is in .png format with a dimension of 224 by 224 pixels.

The dataset consisted of 770 images, which was considered to be insufficient for training deep learning models effectively. In order to increase the size of the dataset, data augmentation was carried out to produce additional image files. The enhanced dataset now has 2,671 images overall, with 500 images each class. While maintaining the dataset's diagnostic integrity, methods such as rotation, flipping, and brightness modifications were employed to expand its size and diversity. Details of the datasets are described in Table 2.

Table 2. Dataset description

Class label name	Original image	Augmented image
Chickenpox	107	508
Measles	91	591
Monkeypox	279	779
Normal	293	793
Total	770	2671

The dataset has been curated based on some specific priorities that ensure the quality and usability of the same. It also focuses on visual clarity with high-resolution images, diagnostic relevance by choosing only those images that display features related to each disease, and diversity by incorporating different variations in terms of skin tones, lesion size, and severity to make the model as generalizable as possible.

4.3. Performance Metrics

This part covers the performance measures for classification, starting with Equations (3) through Equations (8). The common measures used for classification are accuracy indicated as A [32], Categorical Cross Entropy indicated as (CCE) [38], binary cross entropy [38], precision [10], recall [10], and F1-score [10].

$$A = \frac{The\ count\ of\ accurately\ detected\ pixels}{The\ images\ total\ pixel\ count} \tag{3}$$

$$CCE = -\sum_{c=1}^{N} y_c\, log(p_c) \tag{4}$$

$$BCE = -\frac{1}{N}[\sum_{j=1}^{N}(t_j(log(p_j)) + (1-t_j)\, log(1-P_j))] \tag{5}$$

$$Precision = \frac{TP}{(TP+FP)} \tag{6}$$

$$Recall = \frac{TP}{(TP+FN)} \tag{7}$$

$$F1\ Score = \frac{2*(Precision*Recall)}{(Precision+Recall)} \tag{8}$$

The accuracy, precision, recall, and *F*1*score* were derived using the confusion matrix. In this context, *TP* denotes the true positive value, while *FN* signifies the false negative value. The confusion matrix will serve as the foundation for all metrics.

In the context of *CCE*, *N* represents the total number of classes included in the model. The variable y_c denotes the true label for class *i*, while pc signifies the probability associated with the predicted classes. In the context of binary cross-entropy (BCE), *N* represents the total count of data points. The variable t_j indicates the truth value associated with the selection of either 1 or 0, while p_j signifies the SoftMax probability corresponding to the j-th data point.

Table 3 provides an overview of the hyperparameter tuning methods that were employed to tune the model. This hyperparameter is applied to both multi-class and binary-class prediction. Only one parameter in this loss changes for binary-class prediction; all other parameters stay unchanged. Binary_cross_entropy was used for binary prediction and categorical_cross_entropy for multi-class prediction. The different activation function was applied to the model in that Adam optimization techniques produced a better result. When you compare relu to other activation functions like tanh, sigmoid, and SoftMax, it does better in all but the dense last layer. In both the convolution and dense layers, it does better.

SoftMax is applied in the final layer, where it functions better. Next, we apply different learning rates, such as 0.01, 0.001, and 0.0001, to the network. In this case, 0.0001 yields a superior outcome. Typically, models employ dropout layers to reduce overfitting. Specifically, dropout was trained from 0.1 to 0.5 since 0.1 performs better, and the generalization of images also gets higher. The threshold value for all images determined the PCA value, which yielded 242. Table 3 displays the finalized parameters used in the model.

Table 3. Hyperparameter tunning.

Parameter name	Parameter size
Optimizer	Adam
Epoch	100
Loss (multi-class)	categorical_crossentropy
Loss (binary)	Binary_crossentropy
Learning rate	0.0001
Activation	Relu, SoftMax
Dropout	0.1
PCA	249
TMF (low, medium, and high)	0, 0.5, 1

Table 4 presents a comparative analysis of benchmark methods. This table compares various benchmark methods, including VGG16, CNN, and ResNet50. This table shows that VGG16 achieves a significantly higher level of image generalization, prompting us to adopt this method for further improvement. When compared to other methods, the VGG16 extraction of global features from images performs well. In the VGG16, the accuracy was 80.13%, the precision was 79.53%, the recall was 79.57%, and the F1-score was 79.55%. This performance is significantly higher than that of CNN and ResNet50.

Table 4. Comparative analysis of the benchmark methods.

Methods	Accuracy	Precision	Recall	F1-Score
VGG16	80.13	79.53	79.57	79.55
CNN	75.75	75.89	75.64	75.73
Resnet50	56.56	53.48	53.57	53.44
FuzzyPCAVGG16	91.42	91.23	91.31	91.27

Figure 6 illustrates various deep learning approaches and their corresponding measurements. The current approaches of the hybrid method of FuzzyPCAVGG16 data are also displayed. The different parameters, like accuracy, precision, recall, and precision of deep learning methods, are shown. We use these measures to establish the VGG16 method as the foundation for improvement.

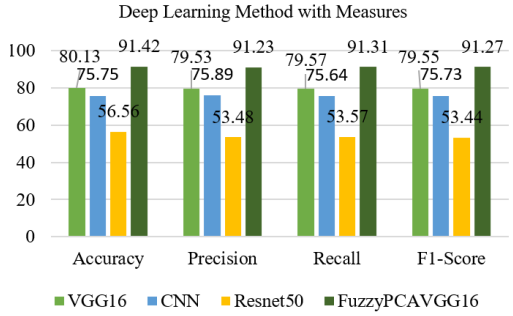

Figure 6. Deep learning method with measures.

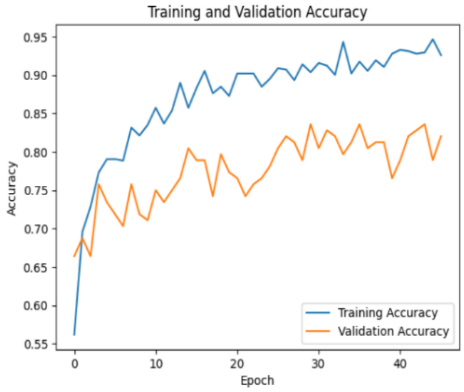

Figure 7. Train and validation accuracy in VGG-16.

Figure 8. VGG16 for train and validation loss.

After 100 iterations, the model was evaluated for accuracy and loss using the VGG-16. The results can be shown in Figures 7 and 8, respectively. At 40 epochs, the network was automatically ended due to incremental validation loss as a result of the early stopping condition. As you can see from the image above, the validation accuracy was low while the training accuracy was high. Indirectly, the fact that the validation loss is high but the training loss is low suggests that the model did a poor job of training and generalising the new images.

The pre-trained model of VGG16 is not able to extract the global information clearly due to the similar and overlapped red bumps. So, the fuzzy techniques were integrated into the model as a layer, after all the convolution and the pooling layer tasks were done. Still the dimensional of the network was high, to reduce this PCA was applied. The fuzzy technique can handle the overlapping data from the images. So, the triangular MF was used. These three variables can be assigned, and different hypotheses are performed to check the network.

Similarly, there was a modest training loss and a significant validation loss. This clearly says that the network has over-fitting issues. The suggested work was used to classify multiple classes. Figure 9 explains their validation and training accuracy. The model received 91.60% for validation and 95.34% for training. Figure 10 shows the losses during training and validation. When comparing the training and validation losses, the current method produces better results than the existing

method.

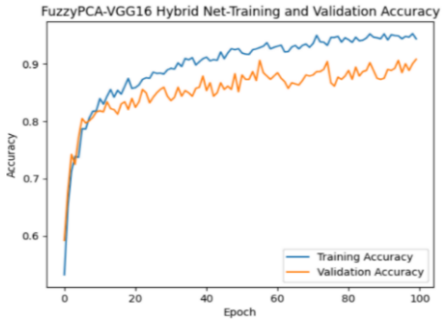

Figure 9. FuzzyPCA-VGG16 hybrid net for training and validation accuracy.

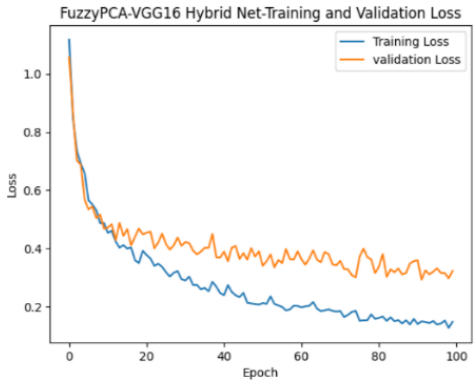

Figure 10. Training and Validation Loss of FuzzyPCA-VGG16 Hybrid Net.

The proposed method was used for binary data classification. The dataset was split into two classes: chickenpox, measles, and normal skin were assigned to one class, and the monkeypox virus was assigned to the other. The loss function used in this model is binary_cross_entropy.

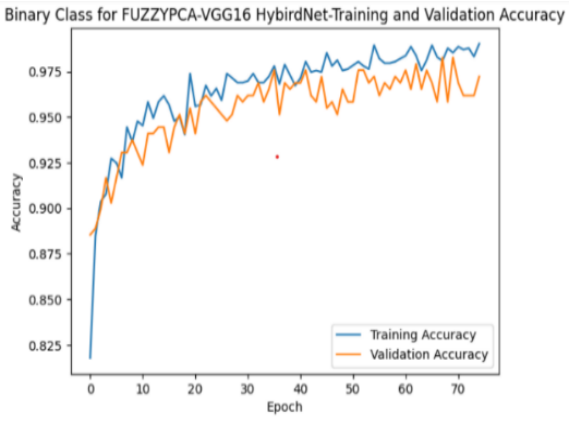

Figure 11. Binary class training and validation accuracy for FuzzyPCA-VGG16 hybrid net.

The model achieved a good level of accuracy in the 70th epoch with the aid of early stopping. Dropout, batch normalization, and learning rate are applied to lessen the overfitting. Figure 11 depicts the FuzzyPCA VGG16 hybrid net's training and evaluation accuracy of 99.02% and 97.22%, respectively. Figure 12 shows the suggested technique's training and validation losses of 2.70% and 8.78%, respectively.

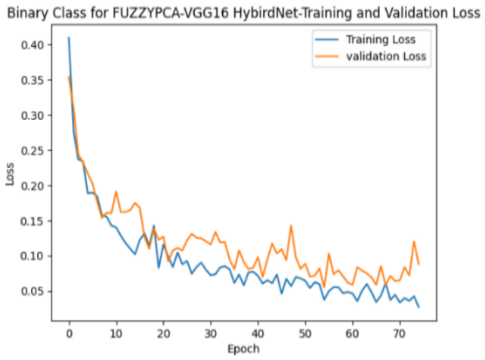

Figure 12. FuzzyPCA-VGG16 hybrid net: binary class training and validation loss.

Table 5. Binary class of FuzzyPCA-VGG16 hybrid net.

Binary class of FuzzyPCA-VGG16 hybrid net		
	Accuracy	**Loss**
Train	99.02	2.70
Test	97.14	6.54
Validation	97.22	8.78

Table 5 and Figure 13 demonstrate the cumulative accuracy and loss of binary class identification. The suggested approach was used for binary classification, The value yielded by them is reflected in the table and chart below. Figure 13 shows the accuracy and loss in binary identification through testing, validation, and training.

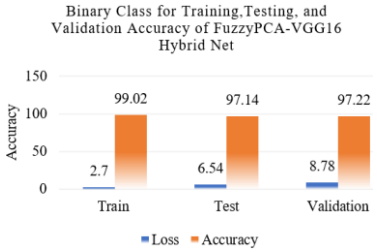

Figure 13. Binary class of FuzzyPCA-VGG16 hybrid net for accuracy and loss.

Table 6. Overall, accuracy for various methods (multi-class).

Accuracy for various methods		
	FuzzyPCA-VGG16 Hybrid Net	**VGG-16**
Train	95.34	92.61
Test	91.42	80.13
Validation	91.60	82.03

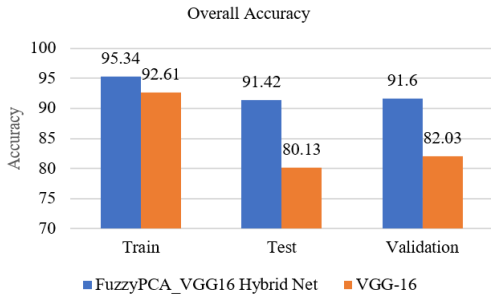

Figure 14. Overall, accuracy chart for various methods.

Table 6 and Figure 14 present the overall accuracy of the VGG-16 method and the FuzzyPCA-VGG 16 Hybrid Net method. The proposed study yields good results when compared to existing approaches,

suggesting that the methods' accuracy in training, testing, and validation is recommended. Both the table and the chart express the multi-class accuracy values.

Table 7. Overall, loss for various methods (multi-class)

	Loss for various methods	
	FuzzyPCA-VGG16 Hybrid Net	**VGG-16**
Train	13.36	20.60
Test	24.59	50.30
Validation	25.39	51.94

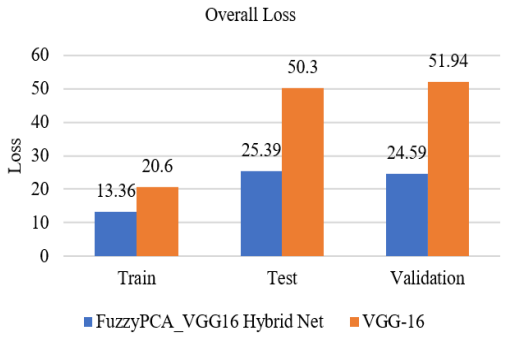

Figure 15. Overall, loss chart for various methods.

The total loss of VGG-16 and the suggested work, which is the FuzzyPCA-VGG16 Hybrid Net approach, are expressed in Table 7 and Figure 15. The suggested work yields a reduced loss rate when compared to the VGG-16 method. Values for multi-class classification loss are displayed in the table and figure.

Table 8. Comparison of existing method and the proposed method.

Authors	**Classes**	**Epoch**	**Accuracy**
Sahin *et al*. [39]	2	60	91.11%
Abdelhamid *et al*. [1]	2	200	98.8%
Ali *et al*. [5]	2	100	82.96%
Ahsan *et al*. [3]	2	100	97%
Yasmin *et al*. [47]	2	30	100%
Sitaula and Shahi [42]	4	16	87.13%
Proposed method (our work)	2	70	97.14%
Proposed method (our work)	4	100	91.42%

Table 8 shows how different individuals classified pox viral disease and human monkeypox sickness using deep neural network approaches. A few contributors have completed multi-class classification; the majority of authors have only completed binary classification. The author employed distinct epochs for both binary-class and multi-class prediction.

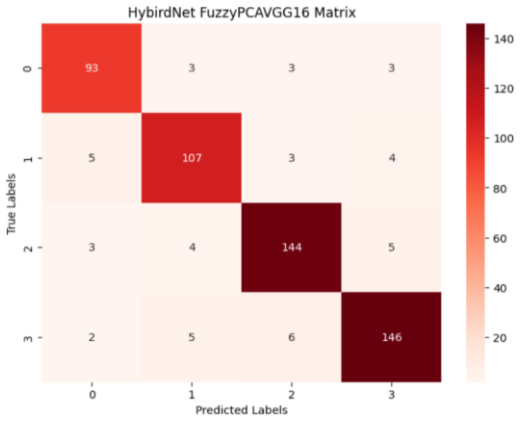

Figure 16. Confusion matrix for FuzzyPCAVGG16.

In Figure 16 the result of the confusion matrix was displayed. The confusion matrix displayed chickenpox as 0, measles as 1, monkeypox as 2, and normal skin as 3. The hybrid method of FuzzyPCAVGG16, the generalisation of chickenpox is 93 out of 102, measles is 107 out of 119, for monkeypox is 144 out of 156, and for normal skin is 146 out of 159.

This section summarizes the overall result with the statistical metrics discussed.

5. Conclusions

Despite the complexities and time demands of multi-class classification arising from overlapping features, the prompt identification of pox virus diseases is essential for effective diagnosis and treatment. This investigation employed a CNN, pre-trained VGG16, Resnet50, model alongside the proposed FuzzyPCA-VGG16 hybrid model to classify pox virus diseases. The proposed model outperformed VGG16, CNN, and Resnet50. We recorded training, testing, and validation accuracies of 95.34%, 91.42%, and 91.6%, respectively, and observed minimal losses during both the training and validation phases. Additionally, when it came to binary classification tasks like figuring out whether monkeypox was present or not, the proposed model did much better than current methods. The findings highlight the efficacy of the proposed model, especially in binary classification contexts where attaining class separability is more manageable. The same proposed work can be applied to any type of image in the real-world application.

5.1. Limitations and Future Works

This effort mainly aimed to categorize images of the pox virus using deep learning techniques. Overfitting occurs due to the limited size and lack of variety in the available datasets, even though there are encouraging outcomes. Future work will address these difficulties by working together to increase datasets, optimizing to decrease overfitting, validating the model in clinical contexts, and integrating explanatory approaches to improve trust and usability. With these updates, we want to make the model more applicable to healthcare settings, increase its clinical diagnostic capabilities, and broaden its applicability.

Acknowledgment

The authors express gratitude to the anonymous reviewers and journal editors for their insightful comments and suggestions.

Data Availability

Kaggle provides the Monkeypox Skin Image Datasets (MSID) benchmark datasets at https://doi.org/10.34740/KAGGLE/DSV/3971903.

References

[1] Abdelhamid A., El-Kenawy E., Khodadadi N., Mirjalili S., Khafaga D., Alharbi A., Ibrahim A., Eid M., and Saber M., "Classification of Monkeypox Images Based on Transfer Learning and the Al-Biruni Earth Radius Optimization Algorithm," *Mathematics*, vol. 10, no. 19, pp. 1-19, 2022. https://doi.org/10.3390/math10193614

[2] Ahad M., Li Y., Song B., and Bhuiyan T., "Comparison of CNN-based Deep Learning Architectures for Rice Diseases Classification," *Artificial Intelligence in Agriculture*, vol. 9, pp. 22-35, 2023. https://doi.org/10.1016/j.aiia.2023.07.001

[3] Ahsan M., Ramiz Uddin M., Farjana M., Sakib A., Al Momin K., and Luna S., "Image Data Collection and Implementation of Deep Learning-based Model in Detecting Monkeypox Disease Using Modified VGG16," *arXiv Preprint*, vol. arXiv:2206.01862v1, pp. 1-14, 2022. https://doi.org/10.48550/arXiv.2206.01862

[4] Albashish D., Al-Sayyed R., Abdullah A., Ryalat M., and Ahmad Almansour N., "Deep CNN Model Based on VGG16 for Breast Cancer Classification," *in Proceedings of the International Conference on Information Technology*, Amman, pp. 805-810, 2021. DOI:10.1109/ICIT52682.2021.9491631

[5] Ali S., Ahmed M., Paul J., Jahan T., Sani S., Noor N., and Hasan T., "Monkeypox Skin Lesion Detection Using Deep Learning Models: A Feasibility Study," *arXiv Preprint*, vol. arXiv:2207.03342v1, pp. 1-4, 2022. https://arxiv.org/abs/2207.03342

[6] Alomar K., Aysel H., and Cai X., "Data Augmentation in Classification and Segmentation: A Survey and New Strategies," *Journal of Imaging*, vol. 9, no. 2, pp. 1-26, 2023. https://doi.org/10.3390/jimaging9020046

[7] Arashova G., "Present Stage Clinical Manifestations of Chickenpox," *International Journal of Medical Sciences and Clinical Research*, vol. 3, no. 8, pp. 64-71, 2023. https://theusajournals.com/index.php/ijmscr/article/view/1607

[8] Azam M., Hasan M., Hassan S., and Abdulkadir S., "Fuzzy Type-1 Triangular Membership Function Approximation Using Fuzzy C-Means," *in Proceedings of the International Conference on Computational Intelligence*, Bandar Seri Iskandar, pp. 115-120, 2020. DOI: 10.1109/ICCI51257.2020.9247773

[9] Barhoom A., Al-Hiealy M., and Abu-Naser S., "Bone Abnormalities Detection and Classification Using Deep Learning-VGG16 Algorithm," *Journal of Theoretical and Applied Information Technology*, vol. 100, no. 20, pp. 6173-6184, 2022. https://www.jatit.org/volumes/Vol100No20/29Vol100No20.pdf

[10] Bauskar S., Madhavaram C., Galla E., Sunkara J., Gollangi H., and Rajaram S., "Predictive Analytics for Project Risk Management Using Machine Learning," *Journal of Data Analysis and Information Processing*, vol. 12, pp. 566-580, 2024. https://papers.ssrn.com/sol3/papers.cfm?abstract_id=5023999

[11] Chadaga K., Prabhu S., Sampathila N., Nireshwalya S., Katta S., Tan R., and Acharya U., "Application of Artificial Intelligence Techniques for Monkeypox: A Systematic Review," *Diagnostics*, vol. 13, no. 5, pp. 1-16, 2023. https://doi.org/10.3390/diagnostics13050824

[12] Chatterjee S., Dey D., and Munshi S., *Recent Trends in Computer-Aided Diagnostic Systems for Skin Diseases: Theory, Implementation, and Analysis*, Elsevier eBooks, 2022. https://doi.org/10.1016/B978-0-323-91211-2.00002-0

[13] Choubey D., Kumar P., Tripathi S., and Kumar S., "Performance Evaluation of Classification Methods with PCA and PSO for Diabetes," *Network Modeling Analysis in Health Informatics and Bioinformatics*, vol. 9, no. 1, pp. 1-30, 2020. file:///C:/Users/user/Downloads/Choubey2019_Article_PerformanceEvaluationOfClassif.pdf

[14] Da Rocha D., Ferreira F., and Peixoto Z., "Diabetic Retinopathy Classification Using VGG16 Neural Network," *Research on Biomedical Engineering*, vol. 38, no. 2, pp. 761-772, 2022. https://link.springer.com/article/10.1007/s42600-022-00200-8

[15] Diponkor B., Kaggle, Monkeypox Skin Images Dataset (MSID), A New Multiclass Skin-based Image Datatset for Monkeypox Disease Detection, https://doi.org/10.34740/KAGGLE/DSV/3971903, Last Visited, 2024.

[16] Dubey A. and Jain V., "Automatic Facial Recognition Using VGG16-Based Transfer Learning Model," *Journal of Information and Optimization Sciences*, vol. 41, no. 7, pp. 1589-1596, 2020. https://doi.org/10.1080/02522667.2020.1809126

[17] Garbin C., Zhu X., and Marques O., "Dropout vs. Batch Normalization: An Empirical Study of their Impact to Deep Learning," *Multimedia Tools and Applications*, vol. 79, no. 19-20, pp. 12777-12815, 2020. https://doi.org/10.1007/s11042-019-08453-9

[18] Goceri E., "Medical Image Data Augmentation: Techniques, Comparisons, and Interpretations," *Artificial Intelligence Review*, vol. 56, pp. 12561-12605, 2023. https://doi.org/10.1007/s10462-023-

10453-z

[19] Griffin D., "Measles Virus Persistence and its Consequences," *Current Opinion in Virology*, vol. 41, pp. 46-51, 2020. DOI:10.1016/j.coviro.2020.03.003

[20] Gunasekaran S. and Vivekasaran S., "Disease Prognosis of Fetal Heart's Four-Chamber and Blood Vessels in Ultrasound Images Using CNN Incorporated VGG 16 and Enhanced DRNN," *The International Arab Journal of Information Technology*, vol. 21, no. 6, pp. 1111-1127, 2024. https://doi.org/10.34028/iajit/21/6/13

[21] Haripriya K. and Hannah Inbarani H., "Performance Analysis of Machine Learning Classification Approaches for Monkey Pox Disease Prediction," *in Proceedings of the 6th International Conference on Electronics, Communication, and Aerospace Technology*, Coimbatore, pp. 1045-1050, 2022. DOI: 10.1109/ICECA55336.2022.10009407

[22] Haripriya K. and Hannah Inbarani H., *Congress on Control, Robotics, and Mechatronics*, Springer, 2023. https://link.springer.com/chapter/10.1007/978-981-99-5180-2_18

[23] Hraib M., Jouni S., Albitar M., Alaidi S., and Alshehabi Z., "The Outbreak of Monkeypox 2022: An Overview," *Annals of Medicine and Surgery*, vol. 79, pp. 1-4, 2022. https://pmc.ncbi.nlm.nih.gov/articles/PMC9289401/pdf/main.pdf

[24] Ioffe S. and Szegedy C., "Batch Normalization: Accelerating Deep Network Training by Reducing Internal Covariate Shift," *in Proceedings of the 32nd International Conference on International Conference on Machine Learning*, Lille, pp. 448-456, 2015. https://dl.acm.org/doi/10.5555/3045118.3045167

[25] Jiang Z., Liu Y., Shao Z., and Huang K., "An Improved VGG16 Model for Pneumonia Image Classification," *Applied Sciences*, vol. 11, no. 23, pp. 1-19, 2021. https://doi.org/10.3390/app112311185

[26] Kavitha S. and Inbarani H., *Computational Vision and Bio-Inspired Computing*, Springer, 2021. https://doi.org/10.1007/978-981-33-6862-0_55

[27] Krishnaswamy Rangarajan A. and Purushothaman R., "Disease Classification in Eggplant Using Pre-Trained VGG16 and MSVM," *Scientific Reports*, vol. 10, pp. 1-11, 2020. https://doi.org/10.1038/s41598-020-59108-x

[28] Lalande A., Chen Z., and Pommier T., et al., "Deep Learning Methods for Automatic Evaluation of Delayed Enhancement-MRI, The Results of the EMIDEC Challenge," *Medical Image Analysis*, vol. 79, pp. 102428, 2022. https://doi.org/10.1016/j.media.2022.102428

[29] Misin A., Antonello R., Di Bella S., Campisciano G., Zanotta N., Giacobbe D., Comar M., and Luzzati R., "Measles: An Overview of a Re-Emerging Disease in Children and Immunocompromised Patients," *Microorganisms*, vol. 8, no. 2, pp. 1-16, 2020. https://doi.org/10.3390/microorganisms8020276

[30] Mumuni A. and Mumuni F., "Data Augmentation: A Comprehensive Survey of Modern Approaches," *Array*, vol. 16, pp. 100258, 2022. https://doi.org/10.1016/j.array.2022.100258

[31] Nalepa J., Marcinkiewicz M., and Kawulok M., "Data Augmentation for Brain-Tumor Segmentation: A Review," *Frontiers in Computational Neuroscience*, vol. 13, pp. 1-48, 2019. https://doi.org/10.3389/fncom.2019.00083

[32] Nivetha S. and Hannah Inbarani H., "Novel Adaptive Histogram Binning-based Lesion Segmentation for Discerning Severity in COVID-19 Chest CT Scan Images," *International Journal of Sociotechnology and Knowledge Development*, vol. 15, no. 1, pp. 1-35, 2023. http://doi.org/10.4018/IJSKD.324164

[33] Nivetha S. and Hannah Inbarani H., "Novel Architecture for Image Classification Based on Rough Set," *International Journal of Service Science, Management, Engineering, and Technology*, vol. 14, no. 1, pp. 1-38, 2023. http://doi.org/10.4018/IJSSMET.323452

[34] Ozsahin D., Mustapha M., Uzun B., Duwa B., and Ozsahin I., "Computer-Aided Detection and Classification of Monkeypox and Chickenpox Lesion in Human Subjects Using Deep Learning Framework," *Diagnostics*, vol. 13, pp. 1-14, 2023. https://doi.org/10.3390/diagnostics13020292

[35] Pan Y., Liu J., Cai Y., and Yang X., et al., "Fundus Image Classification Using Inception V3 and ResNet-50 for the Early Diagnostics of Fundus Diseases," *Frontiers in Physiology*, vol. 14, pp. 1-9, 2023. https://doi.org/10.3389/fphys.2023.1126780

[36] Princy S. and Dhenakaran S., "Comparison of Triangular and Trapezoidal Fuzzy Membership Function," *Journal of Computer Science and Engineering*, vol. 2, no. 8, pp. 46-51, 2016. file:///C:/Users/user/Downloads/659-Article%20Text-1193-1-10-20171231.pdf

[37] Priyanka. and Dharmender Kumar., "Feature Extraction and Selection of Kidney Ultrasound Images Using GLCM and PCA," *Procedia Computer Science*, vol. 167, pp. 1722-1731, 2020. https://doi.org/10.1016/j.procs.2020.03.382

[38] Pykes K., Cross-Entropy Loss Function in Machine Learning: Enhancing Model Accuracy, https://www.datacamp.com/tutorial/the-cross-entropy-loss-function-in-machine-learning, Last Visited, 2024.

[39] Sahin V., Oztel I., and Oztel G., "Human Monkeypox Classification from Skin Lesion

Images with Deep Pre-Trained Network Using Mobile Application," *Journal of Medical Systems*, vol. 46, pp. 1-11, 2022. https://doi.org/10.1007/s10916-022-01863-7

[40] Shivadekar S., Kataria B., Hundekari S., Wanjale K., Balpande V., and Suryawanshi R., "Deep Learning Based Image Classification of Lungs Radiography for Detecting COVID-19 Using a Deep CNN and ResNet 50," *International Journal of Intelligent Systems and Applications in Engineering*, vol. 11, no. 1S, pp. 241-250, 2023. https://ijisae.org/index.php/IJISAE/article/view/2499

[41] Shorten C. and Khoshgoftaar T., "A Survey on Image Data Augmentation for Deep Learning," *Journal of Big Data*, vol. 6, pp. 1-48, 2019. https://doi.org/10.1186/s40537-019-0197-0

[42] Sitaula C. and Shahi T., "Monkeypox Virus Detection Using Pre-Trained Deep Learning-based Approaches," *Journal of Medical Systems*, vol. 46, no. 11, pp. 78, 2022. https://doi.org/10.1007/s10916-022-01868-2

[43] The Indian Express logo Journalism of Courage, Why Congo's Latest Mpox Outbreak is Concerning, https://indianexpress.com/article/explained/explained-health/why-congos-latest-mpox-outbreak-is-concerning-9304630/, Last Visited, 2024.

[44] Theckedath D. and Sedamkar R., "Detecting Affect States Using VGG16, ResNet50 and SE-ResNet50 Networks," *SN Computer Science*, vol. 1, no. 2, pp. 79, 2020. https://link.springer.com/article/10.1007/s42979-020-0114-9

[45] Wang S., Khan M., Hong J., Arun Kumar S., and Zhang Y., "Alcoholism Identification Via a Convolutional Neural Network Based on Parametric ReLU, Dropout, and Batch Normalization," *Neural Computing and Applications*, vol. 32, pp. 665-680, 2020. https://doi.org/10.1007/s00521-018-3924-0

[46] Yang S., Xiao W., Zhang M., Guo S., Zhao J., and Shen F., "Image Data Augmentation for Deep Learning: A Survey," *arXiv Preprint*, vol. arXiv:2204.08610v2, pp. 1-8, 2023. https://arxiv.org/abs/2204.08610

[47] Yasmin F., Hassan M., Hasan M., Zaman S., Kaushal C., El-Shafai W., and Soliman N., "PoxNet22: Fine-Tuned Model for the Classification of Monkeypox Disease Using Transfer Learning," *IEEE Access*, vol. 11, pp. 24053-24076, 2023. DOI:10.1109/ACCESS.2023.3253868

K.P. Haripriya received her MCA from Kumaraguru College of Technology, Anna University, Coimbatore, India, in 2018. She is currently pursuing a Ph.D. as a Research Scholar in the Department of Computer Science at Periyar University, Salem, Tamil Nadu, India. She qualified for the UGC NET-JRF in June 2023. Her research interests include image processing, machine learning, and deep learning.

H. Hannah Inbarani received her M.Sc. from Bharathidasan University, Trichy, India, in 1991, her M.Phil. from M.S. University, Tirunelveli, India, in 2003, and her MTech. degree from AAI University, Allahabad, India, in 2006, and her Ph.D. from Periyar University, Salem, India, in 2012. She is a Professor of Computer Science at Periyar University, Salem, Tamil Nadu, India. She completed a UGC major research project in 2016 and mentored a DST-NASI project, which was completed in 2015. She has received five Best Research Awards at various regional, national, and international conferences. She has authored and co-authored more than 110 papers in international journals. Her research interests include machine learning, deep learning, image processing, signal processing, and bioinformatics. She is the corresponding author of this paper.